Plant Physiology and Biochemistry 122 (2018) 10–18

Contents lists available at ScienceDirect

Plant Physiology and Biochemistry

journal homepage: www.elsevier.com/locate/plaphy

Research article

Transcriptome profiling reveals specific patterns of paclitaxel synthesis in a new *Taxus yunnanensis* cultivar☆

Chun-Tao He[a], Zhi-Liang Li[b], Qian Zhou[a,c], Chuang Shen[a], Ying-Ying Huang[a], Samavia Mubeen[a], Jun-Zhi Yang[d], Jian-Gang Yuan[a], Zhong-Yi Yang[a,*]

[a] State Key Laboratory for Biocontrol, School of Life Sciences, Sun Yat-Sen University, Guangzhou 510275, China
[b] MeiZhou ZhongTian Medicinal Research Institute, Meizhou 514021, China
[c] School of Life Sciences, Xiamen University, Xiamen 361005, China
[d] College of Pharmacy, University of Arizona 85721, USA

ARTICLE INFO

Keywords:
Taxus yunnanensis
Paclitaxel
10-Deacetylbaccatin III
Transcriptome
Transcription factor

ABSTRACT

The difference in contents of paclitaxel and 10-deacetylbaccatin III (10-DABIII) in needles between wildtype (WT) and a new cultivar (Zhongdayihao, ZD1) of *Taxus yunnanensis* was examined. Transcriptome profiling was conducted for different tissues of the ZD1 and WT to illustrate the regulation mechanism of paclitaxel biosynthesis. It was observed that average contents of paclitaxel and 10-DABIII in ZD1 were 4 folds and 32 folds higher than those in WT, respectively. More significant elevations of differential expressed genes (DEGs) from paclitaxel biosynthesis pathway were revealed in ZD1 rather than WT, which should be responsible for the higher contents of paclitaxel and 10-DABIII in the ZD1. Special tissues-dependent expression patterns of paclitaxel biosynthesis DEGs in ZD1 compared to WT were unraveled. The relative higher expressions of paclitaxel biosynthesis genes in needles than other tissues supported the higher content of paclitaxel and 10-DABIII content in needles of ZD1. Attenuation of plant hormone signal transduction pathway led to the lower expression of TFs in ZD1 rather than WT. Besides, the significant negative correlations between differential expressed TFs and DEGs from paclitaxel biosynthesis pathway displayed a possibly negative regulation pattern of these TFs on paclitaxel biosynthesis pathway genes. These results provided new insights into the molecular process of paclitaxel synthesis in *Taxus*.

1. Introduction

Paclitaxel is one of the most effective anticarcinogens for cancers such as breast and ovarian, which was approved by the United States Food and Drug Administration (FDA) (Croteau et al., 2006). The ongoing increase in cancer incidence rates has boosted market demands of the intermediates (10-deacetylbaccatin III, 10-DABIII) as well as paclitaxel (Jennewein and Croteau, 2001). More than 14 species of the *Taxus* genus have been identified so far, and the barks and roots of some *Taxus* species have been the main natural sources of paclitaxel and 10-DABIII (Croteau et al., 2006). Alternative methods such as *in vitro Taxus* cell culture have been developed to obtain paclitaxel and 10-DABIII (Arnone et al., 2006), but most of these methods are difficult to industrialize due to their high cost and low production rate (Kusari et al., 2014). A breakthrough was achieved in the *in vitro* synthesis of paclitaxel through plant cell fermentation and also partly relieved the need for 10-DABIII in the production of docetaxel. However, the need for paclitaxel and 10-DABIII is not eliminated yet due to the increasing incidences of cancer. *Taxus* yews thus still remained an ideal and reliable source for paclitaxel and other precursors. As a result, most *Taxus* species have encountered continuous destruction due to the over-exploitation (Burgarella et al., 2012), and all species of *Taxus* yew have been listed as species for first-grade protection in the National Key Protected Wild Plants List in China consequently (Yu, 1999). Therefore, exploring a method to effectively obtain 10-DABIII and paclitaxel from *Taxus* plants without destroying the population resources is an urgent task for the protection of *Taxus* from the endangerment.

For the purpose, some studies to clarify the biosynthesis mechanisms of paclitaxel have been attempted (Bonfill et al., 2003; Chau and Croteau, 2004; Koksal et al., 2011; Long et al., 2008). Several transcription factors (TFs) families such as MYC, ERF and WRKY have been found to participate in the regulation of paclitaxel biosynthesis (Hartmann et al., 2005; Lenka et al., 2015; Li et al., 2012; Zhang et al., 2015). However, TFs from the same TFs family play different roles in

☆ The nucleotide sequence reported in this paper has been submitted to the Sequence Read Archive (SRA) database of NCBI with the accession number of SRX1176252.

* Corresponding author.
E-mail address: adsyzy@mail.sysu.edu.cn (Z.-Y. Yang).

https://doi.org/10.1016/j.plaphy.2017.10.028
Received 16 September 2017; Received in revised form 30 October 2017; Accepted 30 October 2017
Available online 15 November 2017
0981-9428/

Abbreviation

10-DABIII	10-deacetylbaccatin III
dbat	10-deacetylbaccatin III 10-O-acetyltransferase
tm10bh	5-α-taxadienol-10-β-hydroxylase
bapt	baccatin III 3-animo-3-phenylpropanoyl transferase
bhlh	basic helix-loop-helix
dbnbt	C13-side-chain N-benzoyltransferase
DEGs	differential expressed genes
TFs	transcription factors
ts	taxadiene synthase
tat	taxadiene-5-α-ol O-acetyltransferase
t5oh	taxadiene 5-α-hydroxylase
t13oh	taxane 13-α- hydroxylase
tbt	taxane 2-α-O-benzoyltransferase
t14oh	taxane 14-β-hydroxylase
ZD1	Zhongdayihao
WT	wild-type

regulating the biosynthesis in paclitaxel. For example, TcERF12 and TcERF15 were identified as negative and positive regulators in the expression of taxadiene synthase (*ts*) gene (Zhang et al., 2015). The remarkable divergence of TFs has led to the difficulty in understanding the regulation mechanism of paclitaxel biosynthesis. Thus, the regulation roles of TFs in paclitaxel biosynthesis in *Taxus* plants remain to be elucidated. However, the exploit on the regulation pattern of paclitaxel biosynthesis is confronted due to the lack of genomic information and effective molecular tools (Wu et al., 2011).

In 2014, a cultivar named Zhongdayihao (ZD1) with high contents of paclitaxel and 10-DABIII in not only barks and roots, but also needles was registered as a Protecting Plant Variety (20140110) as a result of a continuous investigation and selection upon a wild population of *T. yunnanensis*. However, the contents of other metabolites such as baccatin were relatively low in ZD1. Thus, ZD1 is ideal source for investigating the mechanisms of paclitaxel biosynthesis. In the present study, wildtype (WT) and ZD1 of *T. yunnanensis* were used to investigate their transcriptional differences. Candidate genes that influenced the paclitaxel and 10-DABIII contents were identified. Transcriptome profiles were employed to inspect the differential expression patterns of the paclitaxel synthesis pathway in different tissues between WT and ZD1 of *T. yunnanensis*. By comparing the differences in transcript profile between WT and ZD1, it is hopeful to find out the regulation pattern in the biosynthesis of paclitaxel in *Taxus* plants. This is the first study to illustrate the synthesis pathways of paclitaxel and 10-DABIII on the basis of the transcriptome profile of a new *Taxus* cultivar with high paclitaxel and 10-DABIII contents in needles.

2. Materials and methods

2.1. Plants of WT and ZD1

Plants of WT and ZD1 had been cultivated under the same maintenance in the fields of Songkou town of Meizhou, Guangdong, China (116°16′E, 40°01′N) since 2008. ZD1 was a cultivar selected from the population of *T. yunnanensis* in 1997 by monitoring the production of paclitaxel and 10-DABIII. For cultivating stage, the individuals of ZD1 and WT at the same age were cultivated closely and under the same management condition such as sunshine controlling method and water management. Long-term monitoring of paclitaxel and 10-DABIII contents of needles in the WT and ZD1 was conducted every year.

2.2. Samplings

Needle samples of WT and ZD1 were simultaneously collected as contrasts from 2004 to 2014. Each of the collected sample was cleaned and stocked in a plastic bag for paclitaxel and 10-DABIII determinations.

On October 2014, needles, branches and root samples of WT and ZD1 with the same age (21-year-old) grown under the same cultivating conditions were collected independently for RNA extraction and transcriptome study. Triplicate samples for each tissue (needles and branches from two year branches) were collected from different part of ZD1 while triplicate samples for each tissue were collected from three different WT plants. The collected samples were sheared into small pieces of no longer than 1 cm and stored in RNAlater stabilization solution (Life technology, Thermo Fisher Scientific, USA).

2.3. Paclitaxel and 10-DABIII determination

The measurements of paclitaxel and 10-DABIII were carried out after the samples were collected. The samples were dried at 40 °C for about 4 h to constant weight. The dried samples were further smashed in a pulverizer. Three grams of the resulting powders were weighed with high precision, added with 100 mL of ACE-H_2O (3:2), and stirred at 240 r/min for 60 min for extraction. The supernatant was collected after filtration. The extraction process was repeated four times and the solutions were combined. After elimination of Ace by rotary evaporation, the remaining solutions were extracted with 50 mL DCM for three times. The extracts were dried in vacuum-dryer and stored at 4 °C. Methanol was added to dilute the products to 100 mL in volume. One milliliter of the solutions was used for the paclitaxel and 10-DABIII determination processes after filtered with 0.22 μm filter membrane.

The Shimazu LC-20A system coupled with SIL-20A automatic sampler, CTO-20A column oven, and SPD-M20A photo-diode array detector were applied with an Agilent ZORBAX SB-C18 column (5 μm, 4.6*250 mm). The mobile phase composed of acetonitrile: water (30:70) was isocratically eluted at a flow rate of 1 mL/min under 25 °C. The volume of each injection was 10 μL. Standard solutions of paclitaxel and 10-DABIII were employed to build up the standard curves for quantification.

2.4. RNA extraction

Samples for RNA extraction were stored in the RNAlater buffer at the field for timely extraction of RNA. Total RNA was extracted from 0.5 g samples of different tissues with the RN09-EASY spin plus Plant Kit (Aidlab Biotech, Beijing, China) according to the manufacturer's instruction. DNA contamination was removed during the RNA extraction process. The RNA quality was verified by RNase free agarose gel electrophoresis and the 2100 Bioanalyzer (Agilent Technologies, Santa Clara, CA). High quality RNA samples of the triplicates from different tissues of ZD1 and WT were mixed with equal quantity for the cDNA library construction and the subsequent RNA sequencing. Six mixed RNA samples of needles, branches, and roots of ZD1 and WT were obtained finally.

2.5. cDNA library construction and sequencing

The obtained poly (A) mRNA samples were broken into fragments of approximately 200 nt after isolation of Oligo (dT) cellulose (Qiagen, USA). After fragmentation, the first-strand cDNA was synthesized by reverse transcriptase with random primers, and second-strand cDNA was formed using DNA polymerase I and RNase H. The cDNA fragments were purified using QIAquick PCR Extraction Kit (Qiagen, USA) before end repairing, poly (A)-tailing and ligation to Illumina adapters. Agarose gel electrophoresis was performed for size fraction of the ligation products, and the fragments were excised for PCR amplification

to construct the cDNA library and were sequenced using Illumina HiSeq™ 2000 (pair-end sequencing, length 125 bp) (Illumina Inc., CA, USA).

2.6. De novo transcriptome assembly and annotation

Raw reads containing adapter, reads with more than 5% unknown nucleotides, and low quality reads with over 20% low Q-value (≤10) base were removed by Perl program (version 5.18.4) before assembly. Clean reads of six RNA samples were merged and *de novo* assembled using Trinity Package 2.0 to construct unique consensus sequences as transcriptome reference. The obtained transcripts were annotated by the BLASTx program (version 2.2.29) with an E-value threshold of $1e^{-5}$ to the NCBI nr database (Nr, http://www.ncbi.nlm.nih.gov), the Swiss-Prot protein database (http://www.expasy.ch/sprot) with an e-value cut off of 10^{-5}, Kyoto Encyclopedia of genes and genomes (KEGG, http://www.genome.jp/kegg), and the COG database (http://www.ncbi.nlm.nih.gov/COG). The best alignment results were adopted for further analysis.

2.7. Identification of DEGs

Clean reads of each sample were mapped to reference sequence by the SOPA aligner/soap2 software (version 2.21). Unique mapped reads were obtained with the rule of no more than 2 mismatch bases. The expression level of unigenes was represented by RPKMs (reads per kb per million reads) was adopted to represent the expression level of unigenes by assessing and normalizing the number of unique-match reads which is a promising method to eliminate the influence of different gene lengths and sequencing discrepancies on the gene expression calculation. The samples were compared using DESeq (Abders and Huber). Significant DEGs were identified by the method with stringent false discovery correction as suggested by Rajkumar et al. (2015). The threshold of P-value was determined with false discovery (FDR) ≤0.001 and an absolute value of $\log_2$Ratio ≥ 1.

These DEGs were subjected to Gene Ontology (GO, http://www.geneontology.org/) terms by using Blast2GO (version 2.8) to search the Nr database. GO classification was achieved in WEGO (http://wego.genomics.org.cn/cgi-bin/wego/index.pl) and categorized into the molecular function, biological process, and cellular component. The *p*-values were adjusted with the Bonferroni correction, and a corrected *p*-value≤ 0.05 was identified as significantly enriched GO terms. The KEGG pathway annotation was achieved with BLASTX software against KEGG database. The pathway with an FDR value ≤ 0.05 was recognized as enriched pathways.

2.8. Verification of genes expression

Expressions of 15 randomly selected genes from three biological replicates were determined with actin as reference genes by quantitative real time PCR (qPCR) with three technical replicates on LightCycler 480 (Roche, Basel, Switzerland) with SYBR® Premix Ex Taq II (Tli RNaseH Plus; TAKARA BIO Inc., Shiga, Japan). The real time PCR was carried out in a final volume of 10 μL, which contained 0.5 μL of cDNA. Cycling program was set as the following: initial denaturation at 95 °C for 30 s, 45 cycles of denaturation at 95 °C for 5 s, and annealing and extension at 60 °C for 30 s. A melting curve was obtained at 95 °C for 5s and 60 °C for 1 min followed by continuous heating. Results were analyzed with the integrated LightCycler 480 service software. Relative expressions of the target genes were normalized by the mRNA expression levels of the reference gene *actin*.

2.9. Statistics

The statistics analysis was conducted with SPSS software 18 (SPSS. Inc) for windows. Independent sample *t*-test was operated to compare the paclitaxel and 10-DABIII contents between ZD1 and WT. One-way analysis of variance (ANOVA) was conducted to investigate the chemical contents between needles of different sampling times in ZD1. Spearman correlation was adopted to analyze the relationships between expression levels of differential expression TFs and genes in paclitaxel biosynthesis. Statistical significance was defined as $p < 0.05$. The heatmaps in the figures were accomplished by R package (version 3.1.3, http://www.r-project.org/) and the other figures were made up by Microsoft Office Excel.

3. Results

3.1. Higher contents of paclitaxel and 10-DAB III contents in needles of ZD1

Contents of paclitaxel and 10-DAB III in needles of the collected samples are shown in Fig. 1. Paclitaxel contents in needles of ZD1 ranged from 0.026% to 0.067% (dry weight basis) with a mean value of 0.041%. Mean value of the paclitaxel contents of WT was 0.01% (ranged from 0.005% to 0.015%), only one-quarter of that in ZD1. Significance was detected between ZD1 and WT ($p < 0.001$, Fig. 1A). Decidedly high contents of 10-DABIII, ranging from 0.63% to 0.95% with a mean value of 0.82%, were also found in needles of ZD1, which was about 34 times of that in WT (0.025%) ($p < 0.001$, Fig. 1A). Additionally, no significant difference was observed for the content of paclitaxel as well as 10-DAB III among the needle samples of ZD1 collected from 2011 to 2013 in the same season (Fig. 1B). Similar results were also observed in WT (Table S1).

3.2. De novo sequence assembly of T. yunnanensis

The cDNA libraries of six samples were pooled together to represent the whole transcriptome of *T. yunnanensis*. A total of 120 million clean reads were obtained for the six samples. Clean reads after sequence trimming were merged and *de novo* assembled into 71,479 unigenes as the reference transcripts of *T.yunnanensis*. By remapping to the reference transcripts, 75.13%–81.43% unigenes were identified for the

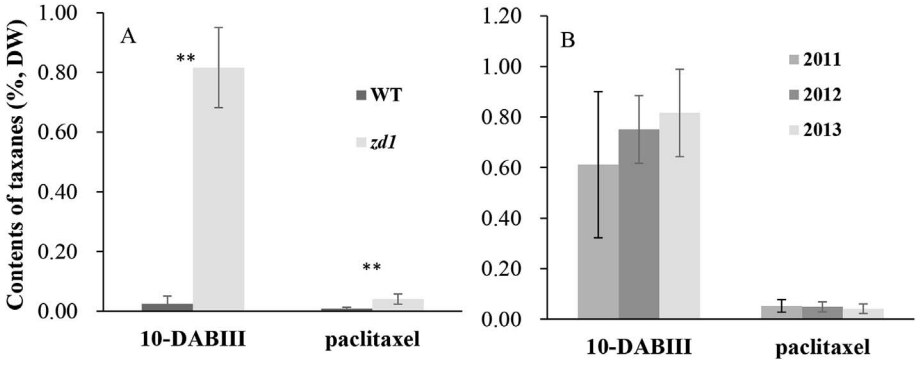

Fig. 1. A. The paclitaxel and 10-DABIII content (dry weight basis) in needle samples of WT and ZD1collected in 2013. **represents significant difference detected between WT and ZD1 for both chemicals at $p < 0.001$. Error bars represent ± standard errors (n = 5). B. Contentsof paclitaxel and 10-DABIII (dry weight basis) in needles of ZD1collected from 2011 to 2013. No significant difference were detected among the three years for both chemicals. Error bars represent ± standard errors (n = 3).

six samples. Summary of the unigenes size distribution is given in Fig. S2. GO classification was performed to annotate unigenes, and cell part (9,310), metabolic process (7,726) and catalytic activity (7,885) were the dominant groups of cellular component, biological process and molecular function, respectively (Fig. S2). Metabolic pathways and biosynthesis of secondary metabolites were the dominant KEGG pathways with 3346 and 1753 unigenes annotated (Table S2). The accession number for raw reads of RNA sequencing were deposited in the Sequence Read Archive (SRA) database of NCBI with the accession number of SRX1176252.

3.3. Gene ontology (GO) and KEGG enrichment analysis of DEGs

In total, 11,579, 12,798 and 19,841 unigenes were identified as DEGs between ZD1 and WT in needles, branches and roots, respectively. The expression levels of the DEGs obtained in transcriptomic sequencing were verified by quantitative PCR of 15 randomly selected DEGs. Similar trends among six samples of the 15 DEGs were observed in the results between qPCR and transcriptomic sequencing (Fig. S3). In addition, a significant correlation was discovered between the two gene expression quantification methods, indicating the reliability in the results of transcriptomic sequencing ($p < 0.01$) (Fig. 2).

Membrane-bounded organelle, catalytic activity and response to stimulus were significant enriched GO terms ($p < 0.05$) with the most DEGs between ZD1 and WT for cellular component, molecular function and biological process, respectively (Table S3). For a preliminary understanding of the molecular mechanism for the high paclitaxel and 10-DABIII contents in needles and branches of ZD1, KEGG classifications were performed for the DEGs between ZD1 and WT in roots, branches and needles (Table 1). The DEGs between ZD1 and WT in different tissues were mainly involved in metabolic pathway, biosynthesis of secondary metabolites (diterpenoid biosynthesis and flavonoid biosynthesis) and precursor of several secondary metabolites (phenylalanine biosynthesis and metabolism) ($p < 0.05$). Among these enriched pathways of DEGs, paclitaxel biosynthesis was a crucial component of the diterpenoid biosynthesis pathway. Apart from the secondary metabolites biosynthesis pathways, some pathways related to signal transduction such as plant hormone signal transduction in needles and plant-pathogen interaction in root were also significantly enriched pathways of the DEGs between WT and ZD1 ($p < 0.05$).

3.4. Enhancement of DEGs involved in the paclitaxel biosynthesis

Paclitaxel biosynthesis, an important part of the diterpenoid biosynthesis, was one of the most significantly enriched pathways in the present study. To further analyze how these DEGs contribute to the higher paclitaxel and 10-DAB III contents in ZD1, DEGs relevant to the paclitaxel biosynthesis pathway were assigned on the basis of RNA-seq data (Fig. 3A). Overall, 101 DEGs were assigned to 10 functional genes in paclitaxel biosynthesis pathway, and the transcript abundances of all these DEGs were significantly higher in the three tested tissues of ZD1 than in those of WT ($p < 0.05$). Among them, *ts* and taxane 13-α-hydroxylase (*t13oh*) were the most significant DEGs in ZD1 which were respectively 4.3–24 folds and 5.6–442 folds higher than those of WT in the three tissues. For other functional genes in paclitaxel synthesis, approximately 6–12 folds, 2–7 folds and 3–4 folds higher transcript abundances were detected in needles, branches, and roots of ZD1 than in those of WT, respectively.

In addition, expression pattern of paclitaxel biosynthesis genes among the tissues of ZD1 was different from that in WT. The expression levels of most DEGs from paclitaxel biosynthesis pathway were ranked in roots » branches > needles or roots » needles > branches in WT (Fig. 3B). In ZD1, however, the expression levels of the DEGs in needles were comparable to those in roots (Fig. 3B). Nevertheless, expressions of DEGs assigned to paclitaxel synthesis pathway of needles were much higher than those of branches in ZD1, which was quite different to the case of WT. Relative elevations in the expressions of most these gene were found in needles of ZD1 which were about 2–5 times of those in branches except taxane 2-α-O-benzoyltransferase (*tbt*).

3.5. Attenuation of DEGs in plant hormone signal transduction pathway

It was found that plant hormone signal transduction pathway was also enriched in addition to the secondary biosynthesis pathways. In total, expression levels of the DEGs participating in plant hormone signal transduction pathway related to abscisic acid (ABA), ethylene and jasmonic acid (JA) in all tissues of ZD1 were lower than those of WT (Fig. 4). Also, carotenoid biosynthesis, α-linolenic acid metabolism and cysteine and methionine metabolism pathways, that are responsible for the ABA, JA and ethylene biosynthesis, were found to be lower expressed in ZD1 than in WT (Table S2). Accordingly, most of the TFs involved in these signal transduction pathways were significantly lower in all tissues of ZD1 when compared to those of WT ($p < 0.05$). Besides, expression levels of differential expressed TFs were ranked in branches > roots > needles in ZD1, while they were in branches > needles > roots in WT. Expression levels of TFs of R2R3-MYB family in WT were 4.8–10.7, 2.1–9.8 and 4.3–5.1 folds of those in ZD1 in needles, roots and branches, respectively, and those in ERF family in WT were 5.5–7.3, 2.2–34.3 and 1.3–6.0 folds of those in ZD1 in the three tissues, respectively. For the TFs in JAMYC family and WRKY family in the three tissues of WT, expressions were 2.3–4.4, 1.4–7.8 and 1.5–5.8 folds, and 3.3–8.4, 1.9–4.4 and 2.6–13.1 folds of those in ZD1, respectively.

3.6. Correlation between the expression of TFs and genes in paclitaxel biosynthesis

To explore the relationship between differential expressed TFs and paclitaxel biosynthesis pathway genes, spearman correlation analysis was adopted (Fig. 5, Table S4). Significant negative correlations ($p < 0.05$) were found between the expressions of the genes encoding TFs and the genes from paclitaxel biosynthesis pathway, including 10-deacetylbaccatin III 10-O-acetyltransferase (*dbat*), 5-α-taxadienol-10-β-hydroxylase (*tm10bh*), baccatin III 3-animo-3-phenylpropanoyl transferase (*bapt*), taxadiene-5-α-ol O-acetyltransferase (*tat*), *tbt*, taxadiene 5-α-hydroxylase (*t5oh*), *t13oh*, taxane 14-β-hydroxylase (*t14oh*), C13-side-chain N-benzoyltransferase (*dbnbt*) and *ts*. About 4 of the 7 differential expressed basic helix-loop-helix (BHLH) domain class TFs and 5 of the 12 differential expressed WRKY TFs were significantly negatively correlated with the DEGs from paclitaxel biosynthesis pathway.

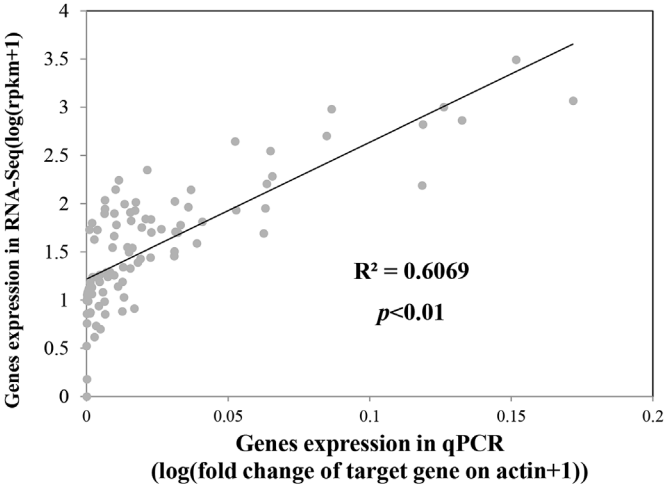

Fig. 2. Correlation between qPCR and RNA sequencing for the 15 randomly selected genes. Each point represents the expression level of selected DEGs in each samples by qPCR and RNA sequencing quantification.

Table 1
KEGG pathway enrichment of DEGs between ZD1 and WT of three tissues. Significant enrichment were identified with Q value < 0.05.

Pathway	DEGs with annotation (2738)	All genes with annotation (12390)	Qvalue	Pathway ID
Needles				
Biosynthesis of secondary metabolites	452 (17.47%)	1753 (14.15%)	0.000	ko01110
Metabolic pathways	794 (30.69%)	3346 (27.01%)	0.000	ko01100
Diterpenoid biosynthesis	114 (4.4%)	147 (1.2%)	0.000	ko00904
Flavonoid biosynthesis	42 (1.62%)	103 (0.83%)	0.000	ko00941
Photosynthesis	39 (1.51%)	112 (0.9%)	0.013	ko00195
Valine, leucine and isoleucine biosynthesis	18 (0.7%)	45 (0.36%)	0.059	ko00290
Plant hormone signal transduction	76 (2.94%)	272 (2.2%)	0.059	ko04075
Phenylalanine metabolism	57 (2.2%)	195 (1.57%)	0.059	ko00360
Phenylpropanoid biosynthesis	84 (3.25%)	310 (2.5%)	0.074	ko00940
Brassinosteroid biosynthesis	14 (0.54%)	34 (0.27%)	0.078	ko00905
Monoterpenoid biosynthesis	8 (0.31%)	18 (0.15%)	0.228	ko00902
Branches				
Phenylpropanoid biosynthesis	111 (4.05%)	310 (2.5%)	0.000	ko00940
Metabolic pathways	852 (31.12%)	3346 (27.01%)	0.000	ko01100
Diterpenoid biosynthesis	108 (4.0%)	147 (1.2%)	0.000	ko00904
Flavonoid biosynthesis	46 (1.68%)	103 (0.83%)	0.000	ko00941
Biosynthesis of secondary metabolites	470 (17.17%)	1753 (14.15%)	0.000	ko01110
Phenylalanine metabolism	71 (2.59%)	195 (1.57%)	0.000	ko00360
Starch and sucrose metabolism	101 (3.69%)	304 (2.45%)	0.000	ko00500
Betalain biosynthesis	6 (0.22%)	7 (0.06%)	0.011	ko00965
Cyanoamino acid metabolism	43 (1.57%)	123 (0.99%)	0.011	ko00460
Other glycan degradation	18 (0.66%)	40 (0.32%)	0.013	ko00511
Flavone and flavonol biosynthesis	17 (0.62%)	37 (0.3%)	0.013	ko00944
Roots				
Ribosome	300 (7.59%)	673 (5.43%)	0.000	ko03010
Phenylpropanoid biosynthesis	157 (3.97%)	310 (2.5%)	0.000	ko00940
Diterpenoid biosynthesis	112 (2.8%)	147 (1.2%)	0.000	ko00904
Flavonoid biosynthesis	62 (1.57%)	103 (0.83%)	0.000	ko00941
Phenylalanine metabolism	100 (2.53%)	195 (1.57%)	0.000	ko00360
Biosynthesis of secondary metabolites	641 (16.22%)	1753 (14.15%)	0.000	ko01110
Starch and sucrose metabolism	128 (3.24%)	304 (2.45%)	0.002	ko00500
Ascorbate and aldarate metabolism	41 (1.04%)	80 (0.65%)	0.004	ko00053
Stilbenoid, diarylheptanoid and gingerol biosynthesis	30 (0.76%)	54 (0.44%)	0.004	ko00945
Phagosome	82 (2.07%)	187 (1.51%)	0.005	ko04145
Glyoxylate and dicarboxylate metabolism	66 (1.67%)	147 (1.19%)	0.008	ko00630

Two JAMYC and two ERF TFs were also significantly negatively correlated to these DEGs.

4. Discussion

4.1. Paclitaxel and 10-DAB III accumulations in ZD1 were much higher than those in the previously investigated experimental lines of Taxus

Barks and roots of *Taxus* plants have been important sources of paclitaxel for industrial productions of medical products. Recently, 10-DABIII, the intermediate product of paclitaxel biosynthesis, is an increasingly important precursor to produce docetaxel (Taxotere) for clinical use. Paclitaxel and 10-DABIII contents in reproducible tissues (especially in needles) of *Taxus* were quite low in previously investigated *Taxus* species, e.g. the maximal values in branches and needles were only 0.021% and 0.017%, respectively in *Taxus* cultivated in China (Zhang et al., 2008). Relatively high 10-DABIII contents (ranged from 0.01% to 0.48%) were measured in the needles of some *T. baccata* cultivars which were also higher than the results of our investigations for WT of *T. yunnanensis* (ranged from 0.008% to 0.06%), and were thus considered as a promising resource of 10-DABIII (van Rozendaal et al., 2000). The facts of the contents of paclitaxel and 10-DABIII in needles of ZD1 being 3 times and 33 times higher than those of WT of *T. Yunnanensis*, which were also preternatural when compared with a lot of published observations (Fu et al., 2009; Vidensek et al., 1990; Wu and Liu, 2013), suggested that ZD1 would be a rare and unusually precious source for production of the medical products of paclitaxel. It has been reported that the content of paclitaxel is sensitive to environmental factors such as cultivation and maintenance measures (Cameron and Smith, 2008; Zhang et al., 2012). In the present study, however, the paclitaxel and 10-DAB III contents in ZD1 were consistent across different growing seasons and different years. It is thus considered that there should be specific biochemical mechanisms as well as molecular processes that impact the paclitaxel and 10-DABIII synthesis in needles of ZD1.

4.2. Paclitaxel biosynthesis of ZD1 were enhanced particularly in needles

The observations that the DEGs between ZD1 and WT of three tissues were enriched in pathways of secondary metabolites biosynthesis, especially in the paclitaxel biosynthesis pathway, suggested that the genotype difference in accumulations of paclitaxel and 10-DABIII were mainly determined by the differed expressions of paclitaxel biosynthesis pathway genes(Patil et al., 2012). Similarly, the strong correlations between the expression level of paclitaxel biosynthesis pathway genes and content of metabolites from paclitaxel biosynthesis pathway were also frequently detected (Hao et al., 2011b; Li et al., 2012; Onrubia et al., 2011a; Sun et al., 2013). Particularly, that expression of *t13oh* in needles of ZD1 was over two order magnitude of the expression levels in WT implied a key point of the mechanisms which were responsible for the high content of paclitaxel and 10-DAB III in needles of ZD1. Further investigation about the regulation of the *t13oh* gene is thus much valuable in further understanding of the paclitaxel biosynthesis.

Interestingly, the difference in 10-DABIII between ZD1 and WT was

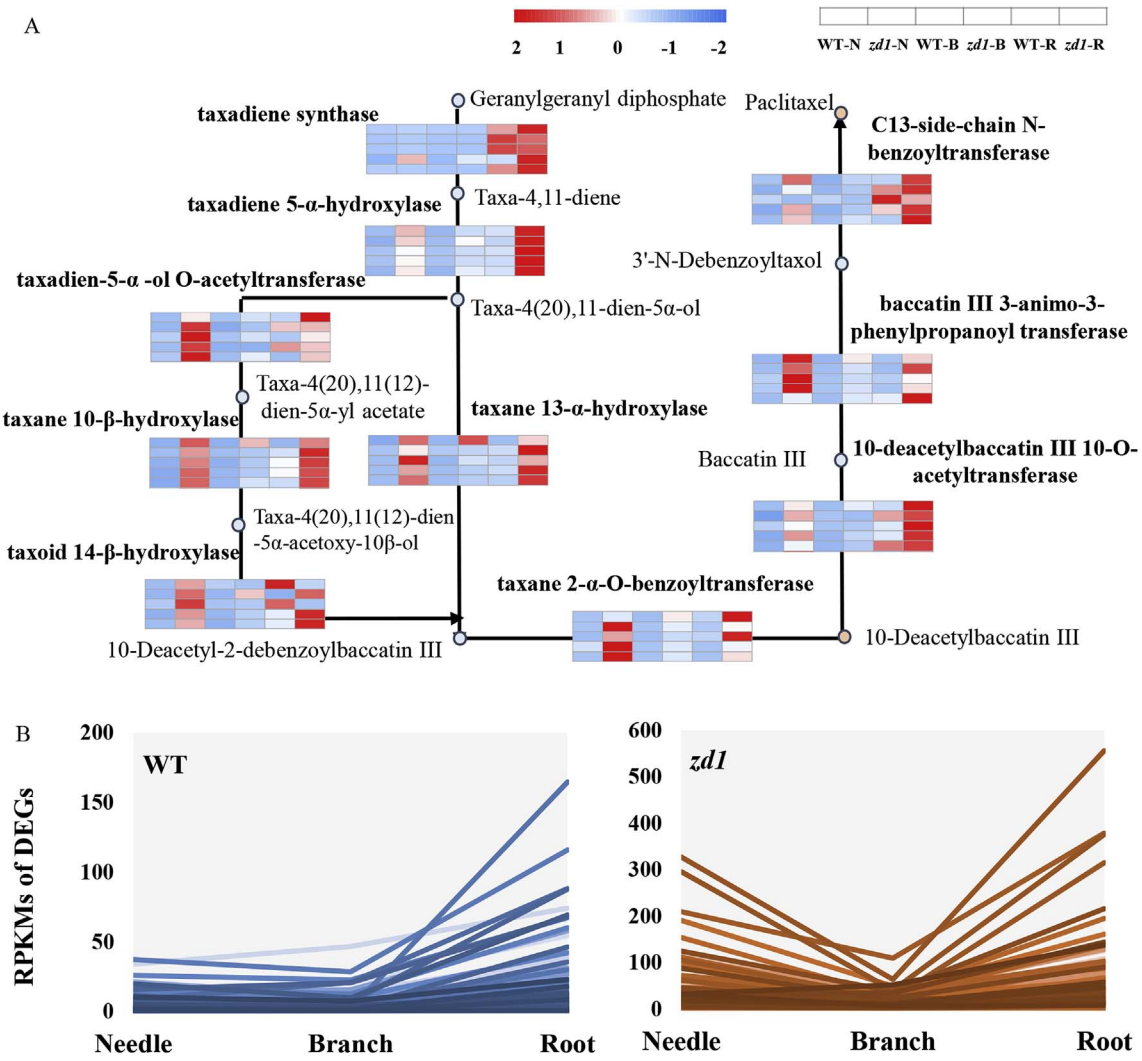

Fig. 3. A. DEGs assigned to paclitaxel biosynthesis pathway and each lane represented the unigene aligned to the target genes. The expression heatmaps from left to right were arranged in the following order: WT-N, ZD1-N, WT-B, ZD1-B, WT-R and ZD1-R. The z-score were applied to represent the fold change among samples. B. Different expression patterns of DEGs involved in paclitaxel biosynthesis pathway among tissues in WT-N and ZD1.

more impressive than paclitaxel. Early study has found out 10-DABIII as the dominant taxane in needles of *T. baccata* (Ghassempour et al., 2009). The remarkable content of 10-DABIII in ZD1 was likely to attribute to the dramatic elevation expression of upstream biosynthesis genes of 10-DABIII, especially *ts* and *t13oh*. What's more, the especially high expressions of upstream biosynthesis genes of 10-DABIII such as *tat* and *tbt* in needles of ZD1, which were even higher than those in roots, probably accounted for the particularly higher 10-DABIII contents than paclitaxel in needles of ZD1. Since the conversion of 10-DABIII to baccatin III was considered as a rate limiting step in the paclitaxel biosynthesis conducted by *dbat* (Katkovcinova et al., 2008; Nasiri et al., 2016; Onrubia et al., 2011b), lower expression of *dbat* rather than upstream genes such as *t13oh* in needles of ZD1 should be a reliable explanation for the lower content of paclitaxel rather than the 10-DABIII.

The finding of the comparative expression levels of paclitaxel synthesis pathway genes between needles and roots of ZD1 was different from the previous report that expressions of genes as well as metabolic activities in roots were higher than those in branches and needles of *T. mairei* (Hao et al., 2011a). In WT, however, the much higher expressions of paclitaxel synthesis pathway genes in root than those in branches and needles were matched the fact of the high paclitaxel accumulation in the root, which has been a well known phenomenon (Hao et al., 2011a; Zhang et al., 2008). Therefore, the expression levels of paclitaxel synthesis pathway genes in needle instead of root or branch were primarily responsible for the high content of paclitaxel and 10-DABIII in needles of ZD1, which was regarded as tissue-dependent expression pattern. A further comparison in the productions of paclitaxel and 10-DABIII between roots and needles in ZD1 is promising.

4.3. Attenuation of plant hormone signal transduction in ZD1 was related to its high paclitaxel and 10-DAB III accumulations in needles

Hormone signal transduction pathways have been determined to be integral in regulating the synthesis of secondary metabolites (Afrin et al., 2015; Akter et al., 2013; Memelink, 2009). JA signal transduction pathway could induce the genes in paclitaxel biosynthesis pathway in *Taxus* spp. cells (Ketchum et al., 2003; Li et al., 2012; Onrubia et al., 2010; Sun et al., 2013). Zhang and Wu (2003) have examined the ethylene inhibitors enhanced paclitaxel production in suspension cultures of *Taxus* spp. cells, indicating the attenuation of ethylene signal transduction could activate the biosynthesis of paclitaxel. However, the results obtained from the present study differed from the above-mentioned studies. Lower expression levels of DEGs participating in plant hormone signal transduction pathway related to ABA, ethylene and JA in different tissues especially in needles of ZD1 than in those of WT suggested an attenuation of plant hormone signal transduction in ZD1.

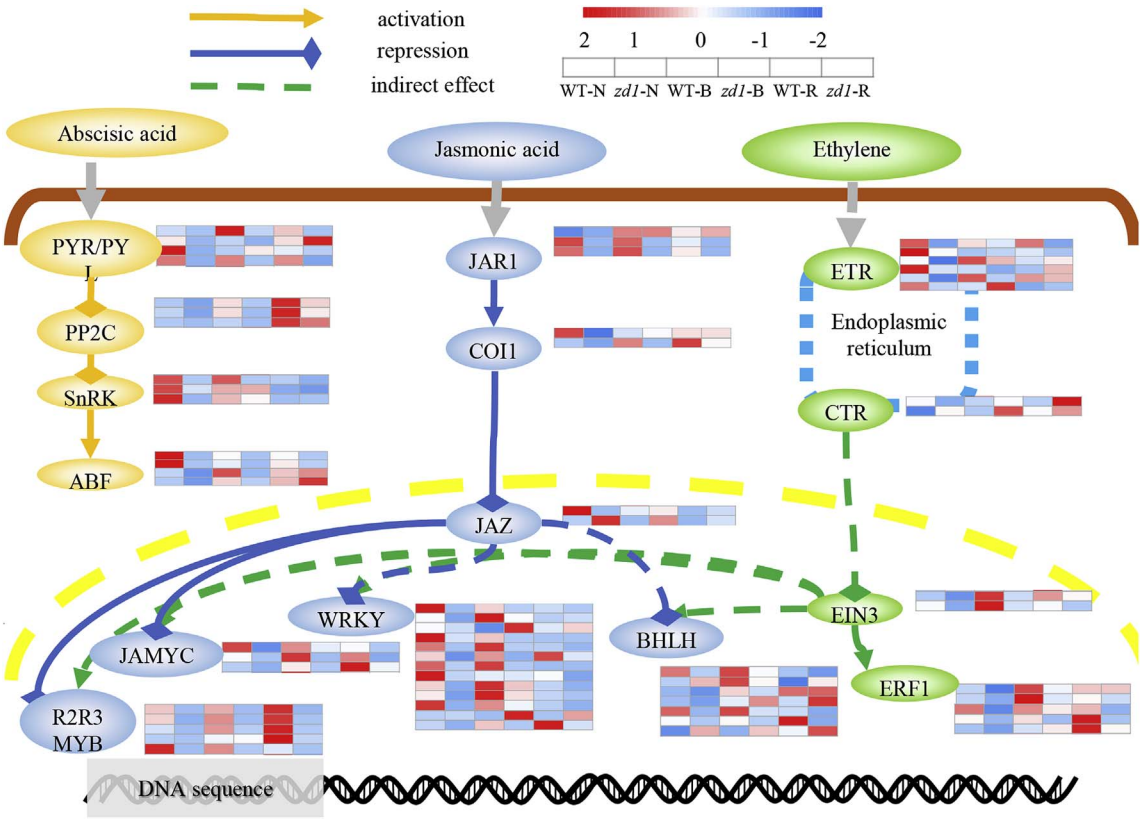

Fig. 4. DEGs assigned to plant hormone signal transduction and each lane represented the unigene aligned to the target genes. The expression heatmaps from left to right were arranged in the following order: WT-N, ZD1-N, WT-B, ZD1-B, WT-R and ZD1-R. The z-score were applied to represent the fold change among samples.

The weakened TFs regulated by plant hormone signal transduction in all three tissues of ZD1 were probably ascribe to the attenuation of plant hormones signal. Also, the decrements in plant hormone generation were consistent with the weakened plant hormone signal transduction. These different observations between our experiment and previous studies might be attributed to the difference between *in vitro* and *in vivo* experimental systems.

4.4. Differential expressed TFs negatively regulated the expressions of paclitaxel biosynthesis DEGs

The positive regulations of TFs such as MYC2, JAMYC, WRKY, ERF, TIFY, R2RE, MYB and bHLH on increasing expression of paclitaxel synthesis genes in *Taxus* cell cultures under MeJA induction suggested that the activation of JA signal transduction could enhance paclitaxel biosynthesis (De Geyter et al., 2012; Lenka et al., 2012; Nims et al.,

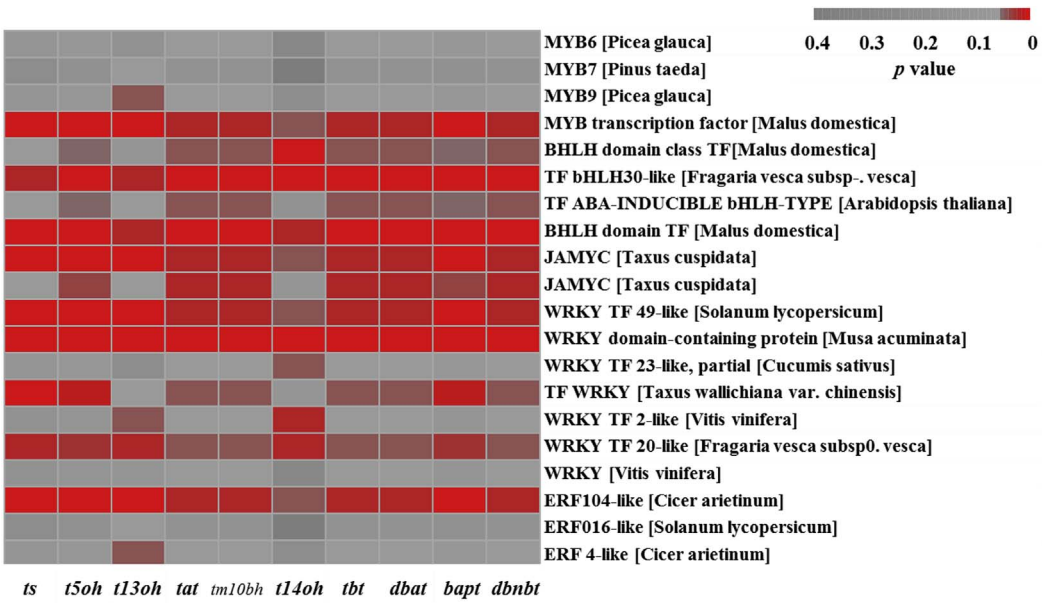

Fig. 5. Correlation between differential expressed TFs and DEGs in paclitaxel biosynthesis pathway (n = 6). Color bar represents the *p* value and significance correlation was detected at $p < 0.05$. (For interpretation of the references to colour in this figure legend, the reader is referred to the web version of this article.)

2006). In the present study, however, there were significant negative correlations between most differential expressed TFs and DEGs from paclitaxel biosynthesis pathway, which proposed the possible negative regulation roles of these TFs on paclitaxel biosynthesis. Negative regulation of TFs as repressor was also reported in other secondary metabolites biosynthesis (Song et al., 2014). For example, a set of R2R3MYBs has been identified as repressors of the phenylpropanoid pathway in *Grapevine* (Cavallini et al., 2015). However, few studies have reported the negative regulation roles of TFs on paclitaxel. Lenka et al. (2015) revealed the possibly negative impacts of TcJAMYC on the paclitaxel synthesis pathway genes after 48 h MeJA elicitation. Zhang et al. (2015) have discovered divergence roles of two ERF TFs, TcERF12 and TcERF15, which act as repressor and activator of *ts* in paclitaxel biosynthesis in *T. chinesis*. Thus, there should be some TFs that function as negative regulators in paclitaxel biosynthesis in *Taxus*.

5. Conclusion

In summary, it was further verified that the new cultivar ZD1 could accumulate much more paclitaxel and 10-DAB III in needles than WT. Expressions of paclitaxel biosynthesis genes were correspondingly significantly much higher in ZD1 than in WT, especially in needles. The tissue-dependent expression patterns of paclitaxel biosynthesis genes in ZD1 were considered to be an important evident to explain the high content of paclitaxel and 10-DABIII in needles. Attenuation of plant hormone signaling in ZD1 has resulted in the decline of TFs from several families such as BHLH, WRKY, ERF and MYC, which might relate to the enhancement in the expressions of paclitaxel biosynthesis genes through a negative regulation of these TFs in ZD1. These observations have revealed a new insight about the regulation roles of TFs on paclitaxel biosynthesis based on the new unusual *Taxus* cultivar. Further study of ZD1 would undoubtedly advance our understanding of the regulation patterns of these TFs and other molecular processes on paclitaxel biosynthesis.

Contributions

Chuntao He and Zhongyi Yang have designed this research. Zhiliang Li was responsible for the sampling and secondary metabolites analysis process. The molecular experiment was carried out by Chuntao He and Chuang Shen. Chuntao He, Qian Zhou, Yingying Huang, and Samavia Mubeen performed the data analysis. Junzhi Yang and Jiangang Yuan assisted with the article revision. The manuscript was finished by Chuntao He and Zhongyi Yang.

Conflict of interest statement

The authors have no conflict of interest to declare.

Acknowledgement

This research was supported by Yangfang Project of Guangdong Province (2014YT02S044) and Science and Technology Planning Project of Guangdong Province, China (2014A070713005) (2016A020208003), and Forestry Science and Technology Innovation Project of Guangdong Province (2017KJCX044).

Appendix A. Supplementary data

Supplementary data related to this article can be found at http://dx.doi.org/10.1016/j.plaphy.2017.10.028.

References

Afrin, S., Huang, J.J., Luo, Z.Y., 2015. JA-mediated transcriptional regulation of secondary metabolism in medicinal plants. Sci. Bull. 60 (12), 1062–1072.

Akter, N., Okuma, E., Sobahan, M.A., Uraji, M., Munemasa, S., Nakamura, Y., Mori, I.C., Murata, Y., 2013. Negative regulation of methyl jasmonate-induced stomatal closure by glutathione in arabidopsis. J. Plant Growth Regul. 32 (1), 208–215.

Arnone, A., Bava, A., Alemani, S., Nasini, G., Bombardelli, E., Fontana, G., 2006. Microbial transformation of 10-deacetylbaccatin III (10-DAB) by Curvularia lunata and Trametes hirsuta. J. Mol. Catal. B-Enzymatic 42 (3–4), 95–98.

Bonfill, M., Palazon, J., Cusido, R.M., Joly, S., Morales, C., Pinol, M.T., 2003. Influence of elicitors on taxane production and 3-hydroxy-3-methylglutaryl coenzyme A reductase activity in Taxus media cells. Plant Physiology Biochem. 41 (1), 91–96.

Burgarella, C., Navascues, M., Zabal-Aguirre, M., Berganzo, E., Riba, M., Mayol, M., Vendramin, G.G., Gonzalez-Martinez, S.C., 2012. Recent population decline and selection shape diversity of taxol-related genes. Mol. Ecol. 21 (12), 3006–3021.

Cameron, S.I., Smith, R.E., 2008. Seasonal changes in the concentration of major taxanes in the biomass of wild Canada yew (Taxus canadensis Marsh.). Pharm. Biol. 46 (1–2), 35–40.

Cavallini, E., Matus, J.T., Finezzo, L., Zenoni, S., Loyola, R., Guzzo, F., Schlechter, R., Ageorges, A., Arce-Johnson, P., Tornielli, G.B., 2015. The phenylpropanoid pathway is controlled at different branches by a set of R2R3-MYB C2 repressors in grapevine. Plant Physiol. 167 (4), 1448–U1552.

Chau, M., Croteau, R., 2004. Molecular cloning and characterization of a cytochrome P450 taxoid 2 alpha-hydroxylase involved in Taxol biosynthesis. Archives Biochem. Biophysics 427 (1), 48–57.

Croteau, R., Ketchum, R.E., Long, R.M., Kaspera, R., Wildung, M.R., 2006. Taxol biosynthesis and molecular genetics. Phytochem. Rev. 5 (1), 75–97.

De Geyter, N., Gholami, A., Goormachtig, S., Goossens, A., 2012. Transcriptional machineries in jasmonate-elicited plant secondary metabolism. Trends Plant Sci. 17 (6), 349–359.

Fu, Y.J., Sun, R., Zu, Y.G., Li, S.M., Liu, W., Efferth, T., Gu, C.B., Zhang, L., Luo, H., 2009. Simultaneous determination of main taxoids in Taxus needles extracts by solid-phase extraction-high-performance liquid chromatography with pentafluorophenyl column. Biomed. Chromatogr. 23 (1), 63–70.

Ghassempour, A., Rezadoost, H., Ahmadi, M., Aboul-Enein, H.Y., 2009. Seasons study of four important taxanes and purification of 10-deacetylbaccatin III from the needles of Taxus baccata L. by two-dimensional liquid chromatography. J. Liq. Chromatogr. Relat. Technol. 32 (10), 1434–1447.

Hao, D.C., Ge, G.B., Xiao, P.G., Zhang, Y.Y., Yang, L., 2011a. The first insight into the tissue specific Taxus transcriptome via Illumina second generation sequencing. PLoS One 6 (6).

Hao, D.C., Yang, L., Xiao, P.G., 2011b. The first insight into the Taxus genome via fosmid library construction and end sequencing. Mol. Genet. Genomics 285 (3), 197–205.

Hartmann, U., Sagasser, M., Mehrtens, F., Stracke, R., Weisshaar, B., 2005. Differential combinatorial interactions of cis-acting elements recognized by R2R3-MYB, BZIP, and BHLH factors control light-responsive and tissue-specific activation of phenylpropanoid biosynthesis genes. Plant Mol. Biol. 57 (2), 155–171.

Jennewein, S., Croteau, R., 2001. Taxol: biosynthesis, molecular genetics, and biotechnological applications. Appl. Microbiol. Biotechnol. 57 (1–2), 13–19.

Katkovcinova, Z., Lazarova, M., Brunakova, K., Kosuth, J., Cellarova, E., 2008. Expression of dbat and dbtnbt genes involved in paclitaxel biosynthesis during the growth cycle of Taxus baccata L. Callus cultures. Zeitschrift Fur Naturforschung Sect. C-a J. Biosci. 63 (9–10), 721–730.

Ketchum, R.E.B., Rithner, C.D., Qiu, D., Kim, Y.S., Williams, R.M., Croteau, R.B., 2003. Taxus metabolomics: methyl jasmonate preferentially induces production of taxoids oxygenated at C-13 in Taxus x media cell cultures. Phytochemistry 62 (6), 901–909.

Koksal, M., Jin, Y.H., Coates, R.M., Croteau, R., Christianson, D.W., 2011. Taxadiene synthase structure and evolution of modular architecture in terpene biosynthesis. Nature 469 (7328), 116–U138.

Kusari, S., Singh, S., Jayabaskaran, C., 2014. Rethinking production of Taxol(R) (paclitaxel) using endophyte biotechnology. Trends Biotechnol. 32 (6), 304–311.

Lenka, S.K., Boutaoui, N., Paulose, B., Vongpaseuth, K., Normanly, J., Roberts, S.C., Walker, E.L., 2012. Identification and expression analysis of methyl jasmonate responsive ESTs in paclitaxel producing Taxus cuspidata suspension culture cells. Bmc Genomics 13.

Lenka, S.K., Nims, N.E., Vongpaseuth, K., Boshar, R.A., Roberts, S.C., Walker, E.L., 2015. Jasmonate-responsive expression of paclitaxel biosynthesis genes in Taxus cuspidata cultured cells is negatively regulated by the bHLH transcription factors TcJAMYC1, TcJAMYC2, and TcJAMYC4. Front. Plant Sci. 6, 115.

Li, S.T., Zhang, P., Zhang, M., Fu, C.H., Zhao, C.F., Dong, Y.S., Guo, A.Y., Yu, L.J., 2012. Transcriptional profile of Taxus chinensis cells in response to methyl jasmonate. Bmc Genomics 13.

Long, R.M., Lagisetti, C., Coates, R.M., Croteau, R.B., 2008. Specificity of the N-benzoyl transferase responsible for the last step of Taxol biosynthesis. Archives Biochem. Biophysics 477 (2), 384–389.

Memelink, J., 2009. Regulation of gene expression by jasmonate hormones. Phytochemistry 70 (13–14), 1560–1570.

Nasiri, J., Naghavi, M.R., Alizadeh, H., Moghadam, M.R.F., 2016. Seasonal-based temporal changes fluctuate expression patterns of TXS, DBAT, BAPT and DBTNBT genes alongside production of associated taxanes in Taxus baccata. Plant Cell Rep. 35 (5), 1103–1119.

Nims, E., Dubois, C.P., Roberts, S.C., Walker, E.L., 2006. Expression profiling of genes involved in paclitaxel biosynthesis for targeted metabolic engineering. Metab. Eng. 8 (5), 385–394.

Onrubia, M., Gallego, A., Ramirez, K., Limon, H.R.V., Cusido, R.M., Bonfill, M., Palazon, J., Moyano, E., 2011a. Changes of taxane production and gene expression during the development of in vitro Taxus plant cultures. Planta Medica 77 (12) 1282–1282.

Onrubia, M., Moyano, E., Bonfill, M., Exposito, O., Palazon, J., Cusido, R.M., 2010. An approach to the molecular mechanism of methyl jasmonate and vanadyl sulphate

elicitation in Taxus baccata cell cultures: the role of txs and bapt gene expression. Biochem. Eng. J. 53 (1), 104–111.
Onrubia, M., Moyano, E., Bonfill, M., Palazon, J., Goossens, A., Cusido, R.M., 2011b. The relationship between TXS, DBAT, BAPT and DBTNBT gene expression and taxane production during the development of Taxus baccata plantlets. Plant Sci. 181 (3), 282–287.
Patil, R.A., Kolewe, M.E., Normanly, J., Walker, E.L., Roberts, S.C., 2012. Contribution of taxane biosynthetic pathway gene expression to observed variability in paclitaxel accumulation in Taxus suspension cultures. Biotechnol. J. 7 (3), 418–427.
Rajkumar, A.P., Qvist, P., Lazarus, R., Lescai, F., Ju, J., Nyegaard, M., Mors, O., Borglum, A.D., Li, Q.B., Christensen, J.H., 2015. Experimental validation of methods for differential gene expression analysis and sample pooling in RNA-seq. Bmc Genomics 16.
Song, S.S., Huang, H., Gao, H., Wang, J.J., Wu, D.W., Liu, X.L., Yang, S.H., Zhai, Q.Z., Li, C.Y., Qi, T.C., Xie, D.X., 2014. Interaction between MYC2 and ethylene INSENSITIVE3 modulates antagonism between jasmonate and ethylene signaling in arabidopsis. Plant Cell 26 (1), 263–279.
Sun, G.L., Yang, Y.F., Xie, F.L., Wen, J.F., Wu, J.Q., Wilson, I.W., Tang, Q., Liu, H.W., Qiu, D.Y., 2013. Deep sequencing reveals transcriptome Re-Programming of Taxus x media cells to the elicitation with methyl jasmonate. PLos One 8 (4).
van Rozendaal, E.L., Lelyveld, G.P., van Beek, T.A., 2000. Screening of the needles of different yew species and cultivars for paclitaxel and related taxoids. Phytochemistry 53 (3), 383–389.
Vidensek, N., Lim, P., Campbell, A., 1990. Taxol content in bark, wood, root, leaf, twig, and seedling from several Taxus species. J. Nat. Prod. 53.
Wu, H.Y., Liu, X.P., 2013. On the determination of content of 10-DABIII in Enshi's Taxus chinensis var mairei. Adv. Mater Res. 821–822.
Wu, Q., Sun, C., Luo, H., Li, Y., Niu, Y., Sun, Y., Lu, A., Chen, S., 2011. Transcriptome analysis of Taxus cuspidata needles based on 454 pyrosequencing. Planta Medica 77 (4), 394–400.
Yu, Y., 1999. The national key protected wild plants in China. Plants 3–11.
Zhang, C.H., Wu, J.Y., 2003. Ethylene inhibitors enhance elicitor-induced paclitaxel production in suspension cultures of Taxus spp. cells. Enzyme Microb. Technol. 32 (1), 71–77.
Zhang, J., Xu, X., Liu, J., Tian, C., Zhou, S., 2008. Study on the taxol distribution in different parts of difference sources Taxus growing in China. Chin. J. Pharm. Anal. 28, 16–19.
Zhang, J., Yang, C.F., Yuan, K., 2012. Simultaneous determination of 10-deacetylbaccatin III, cephalomannine and taxol in different parts of Taxus media with different growth years by UPLC. Mech. Eng. Mater. Sci. 108, 326–330.
Zhang, M., Li, S.T., Nie, L., Chen, Q.P., Xu, X.P., Yu, L.J., Fu, C.H., 2015. Two jasmonate-responsive factors, TcERF12 and TcERF15, respectively act as repressor and activator of tasy gene of taxol biosynthesis in Taxus chinensis. Plant Mol. Biol. 89 (4–5), 463–473.